J Paleolimnol (2007) 37:105–122
DOI 10.1007/s10933-006-9026-5

ORIGINAL PAPER

Sedimentology, clay mineralogy and grain-size as indicators of 65 ka of climate change from El'gygytgyn Crater Lake, Northeastern Siberia

Celeste A. Asikainen · Pierre Francus · Julie Brigham-Grette

Received: 21 June 2004 / Accepted: 1 May 2006 / Published online: 12 December 2006

Abstract El'gygytgyn Crater Lake, NE Siberia was investigated for sedimentological proxies for regional climate change with a focus on the past 65 ka. Sedimentological parameters assessed relative to magnetic susceptibility include stratigraphy, grain size, clay mineralogy and crystallinity. Earlier work suggests that intervals of high susceptibility in these sediments are coincident with warmer (interglacial-like) conditions and well-mixed oxygenated bottom waters. In contrast, low susceptibility intervals correlate with cold (glacial-like) conditions when perennial ice-cover resulted in anoxia and the dissolution of magnetic carrier minerals.

The core stratigraphy contains both well-laminated to non-laminated sequences. Reduced oxygen and lack of water column mixing preserved laminated sequences in the core. A bioturbation index based upon these laminated and non-laminated sequences co-varies with total organic carbon (TOC) and magnetic susceptibility.

Clay mineral assemblages include illite, highly inter-stratified illite/smectite, and chlorite. Under warm or hydrolyzing conditions on the landscape around the lake, chlorite weathers easily and illite/smectite abundance increase, which produces an inverse relationship in the relative abundance of these clays. Trends in relative abundance show distinct down-core changes that correlate with shifts in susceptibility. The mean grain-size (6.92 μm) is in the silt-size fraction, with few grains larger than 65 μm. Terrigenous input to the lake comes from over 50 streams that are filtered through storm berms, which limits clastic deposition into the lake system. The sedimentation rate and terrigenous input grain-size is reduced during glacial intervals. Measurements of particle-size distribution indicate that the magnetic susceptibility fluctuations are not related to grain size.

Lake El'gygytgyn's magnetic susceptibility and clay mineralogy preserves regional shifts in climate including many globally recognized events like the Younger Dryas and Bolling/Allerod. The sedimentary deposits reflect the climatic transitions starting with MIS4 through the Holocene transition. This work represents the first extensive sedimentological study of limnic sediment proxies of this age from Chukotka (Fig. 1).

This is the *eighth* in a series of eleven papers published in this special issue dedicated to initial studies of El'gygytgyn Crater Lake and its catchment in NE Russia. Julie Brigham-Grette, Martin Melles, Pavel Minyuk were guest editors of this special issue.

C. A. Asikainen (✉) · P. Francus · J. Brigham-Grette
Department of Geosciences, University of Massachusetts, Amherst, MA 01003, USA
e-mail: celeste@geo.umass.edu

P. Francus
Centre Eau, Terre et Environnement, Institut national de la recherche scientifique, Québec, QCG1K 9A9, Canada
e-mail: pierre_francus@inrs-ete.uquebec.ca

Keywords Paleoclimate · Grain-size · Clay mineralogy · Lake sediment · Sediment structure

Introduction

Climate variability is the current focus of paleoclimate research, specifically the heterogeneity of regional responses to global-warming. This net trend towards a warmer planet is seen most dramatically in the arctic region, where climate change is expected to be more rapid and severe compared to elsewhere on Earth (Perren et al. 2003). The sensitivity of the arctic region to climate changes is due to several positive feedback

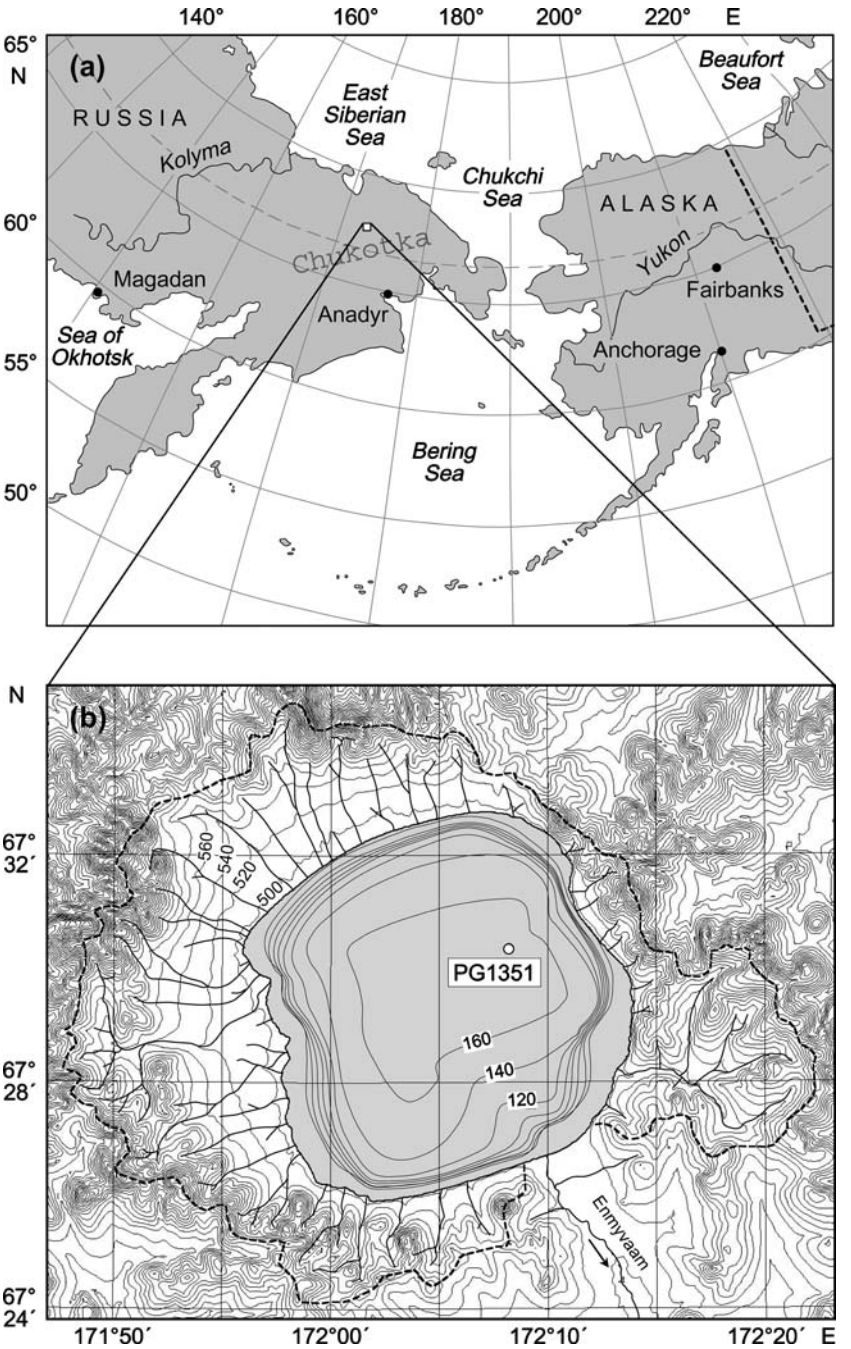

Fig. 1 Location of El'gygytgyn Crater Lake, NE Russia 100 km north of the Arctic Circle and lake morphology

mechanisms that can amplify the warming signal (Imbrie et al. 1993). A decrease in the extent of snow, lake ice, clouds, changes in high latitude solar insolation, and sea ice cover will lower the albedo and enhance warming in this region (Overpeck et al. 1997). It is the sensitivity to climatic change that allows this region to presage climate change at lower latitudes.

Lake sediments are commonly used to infer climate variation through clay mineral assemblages, clay mineral preservation, grain-size, and sediment structures (Chamley 1989; Gale and Hoare 1991; Ariztegui et al. 2001; Yuretich et al. 1999). The clay minerals that are common to arctic environments include illite, smectite, chlorite, and illite/smectite as mixed-layered clay (Chamley 1989). It has been shown that shifts in the relative abundances of these minerals may correlate with glacial/interglacial transitions (Chamley 1989; Velde 1995; Müller 2000; Moore and Reynolds 1989). Additionally, the crystallinity of the clay mineral illite is an environmental monitor that has been used by others to trace changes in temperature as it relates to the hydrolyzing capacity of the depositional environment (Chamley 1989; Blaise 1989; Moore and Reynolds 1989).

In large arctic lacustrine environments, as in Lake El'gygytgyn, depositional patterns are controlled by a number of transport mechanisms including aeolian, turbid underflows, fluvial inflows, and lake ice-rafted debris (Last 2001). These depositional mechanisms can be revealed by particle-size distribution (Gale and Hoare 1991). Further, the analysis of sedimentary units sheds light on depositional environments and can be extended to climatic interpretations. For example, shifts between laminated and non-laminated sequences can be linked (in the right settings) to globally significant changes (Behl 1995). As one of a network of lake systems being studied across the circumarctic, the purpose of this study is to add critical knowledge concerning the sensitivity of Northeastern Asia to global climatic change (Anderson et al. 2002; Hu and Shemesh 2003).

This paper addresses the sedimentological data collected from Lake El'gygytgyn core PG1351 (Fig. 1). These data are corroborated with other proxies in this issue and with a chronology presented by Nowaczyk et al. (2007). In this study we investigate the clay mineralogy, grain-size distribution, and sediment textures. Our goal is to determine whether the sediments of Lake El'gygytgyn preserve a climate signal useful for paleoclimate reconstruction.

Background and chronology

In May 1998, PG1351 core was collected at 175 m depth from the center of the lake. A composite sequence for the 1,300 cm core was constructed based on the physical, biochemical and paleomagnetic properties among the overlapping segments of the core. The depths of this sequence are referred to hereafter as composite depths (Brigham-Grette et al. 2007).

The chronology of the Lake El'gygytgyn record is based on the correlation of the magnetic susceptibility to the GRIP $\delta^{18}O$ curve and magnetic event stratigraphy as measured by Nowaczyk was described in Nowaczyk et al. (2002). Constraints for the age estimates are done by infrared-stimulated luminescence (IRSL) (Forman et al. 2007). Details for the current tuning of this record and the paleomagnetic analyses and age model are based on correlation of magnetic susceptibility with TOC, TiO_2 and regional isolation (Nowaczyk et al. 2007). Additionally, chronology constraints are corroborated by geochemical (Minyuk et al. 2007), biogeochemical (Melles et al. 2007), and pollen (Lozhkin et al. 2007) analyses.

Nowaczyk et al. (2007), shows that high susceptibility in El'gygytgyn Lake sediments correlates with warm, interglacial conditions and higher sedimentation rates. During the ''interglacials'' open water conditions allow for full mixing of the water column providing more oxygen-rich bottom waters. Low susceptibility is thought to correlate with cold (glacial) periods when perennial ice-cover retards mixing of the water column causing anoxic sediment, which results in the dissolution of magnetic carrier materials. Therefore, the nearly two orders of magnitude variation in magnetic susceptibility is thought to reflect the climatic and environmental history of northeastern Siberia over several glacial/interglacial cycles.

Here we report the results of sedimentological analyses completed from Lake El'gygytgyn. The

analyses were done in two stages. (1) The full (1998) 1,300 cm core (~250 ka) was examined for variations in magnetic susceptibility that relate to different sedimentary units (Fig. 2). A low resolution (10–20 cm) sampling of clay mineralogy and grain-size was completed to locate major shifts. (2) From the upper 300 cm, a series of high resolution (2 cm) clay mineralogy and grain-size analyses were completed to determine if significant changes occurred over the past ~65 ka (Fig. 3).

Field area

Lake El'gygytgyn, in the Chukokta region of Northeastern Siberia, is located in a pristine meteorite impact depression about 200 km south of the Arctic Ocean (Fig. 1). The impact occurred ~3.6 Ma (Layer 2000), generating a crater roughly 18 km in diameter. The resulting crater now contains a lake 12 km in diameter (Belyi 1982; Belyi and Chereshnev 1993; Belyi et al. 1994). Following the impact the depression filled with water, initiating the accumulation of over 360 m of sediment (Niessen et al. 2007) in an unglaciated region of Arctic Russia.

The lake is surrounded by rocks of the Late Cretaceous Okhotsk-Chukokta volcanic belt sequence, characterized by felsic lavas, ignimbrites, tuffs, and basalts (Belyi 1982; Belyi and Chereshnev 1993; Layer 2000).

Lake El'gygytgyn's surface lies at ~500 m a.s.l and drains into the Enmyvaam River to the southeast. There are nearly 50 small inlet streams that flow into the lake from a catchment restricted to the 600–900 m crater rim. Abundant geomorphic and seismic data confirm higher lake levels in the past, which are supported by the presence of well-defined terraces that rise at elevations of 6, 12, 18, and 40 m above lake level (Glushkova and Smirnov 2007). Earlier work by Glushkova (1993) showed that the Enmyvaam River has been down-cutting the outlet since impact.

In the 2000 field season we began to understand the modern sedimentary processes occurring in this lake system. Beaches that surround the lake range in width from a few meters to over

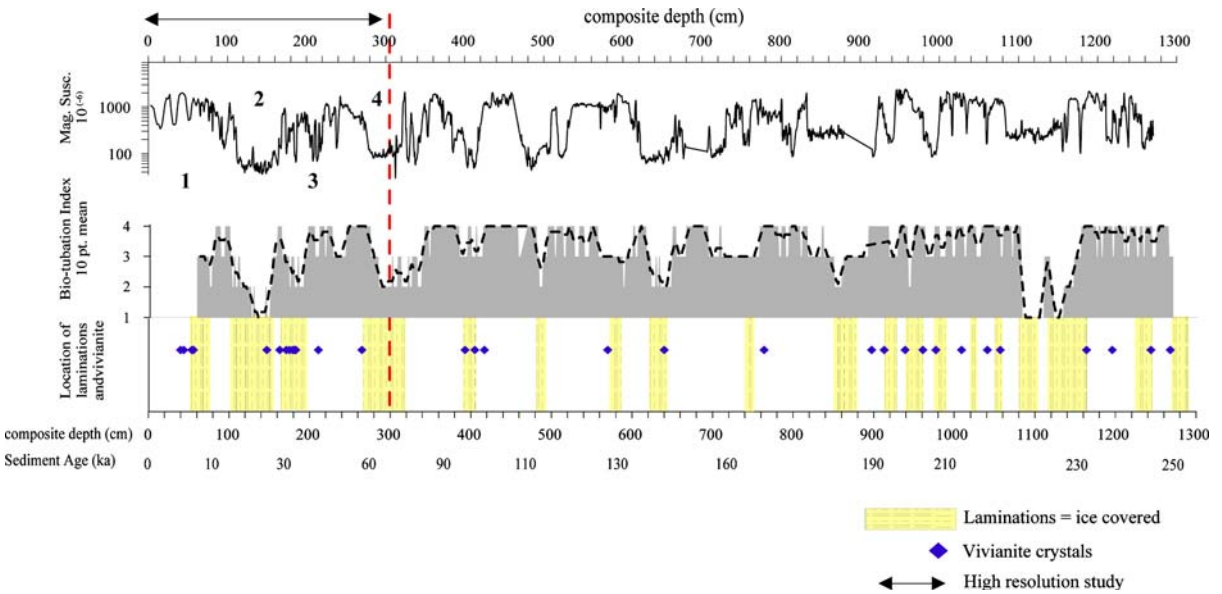

Fig. 2 Magnetic susceptibility (MS) record with depth of the complete 1,300 cm-long core from Lake El'gygytgyn is compared to the bioturbation index, laminated units of the core and occurrences of vivianite. The semi-quantitative bioturbation index is estimated according to Behl and Kennet (1996) at 1 cm resolution (shown with and without a 10 point-mean). The on–off variation in laminated versus non-laminated units illustrates the pattern of sedimentation in Lake El'gygytgyn during several glacial-interglacial cycles. The age model shown below sediment depth and marine isotope stages (shown above and below MS for the upper 300 cm) are tuned to precession-driven changes in North Hemisphere insolation (Nowaczyk et al. 2007)

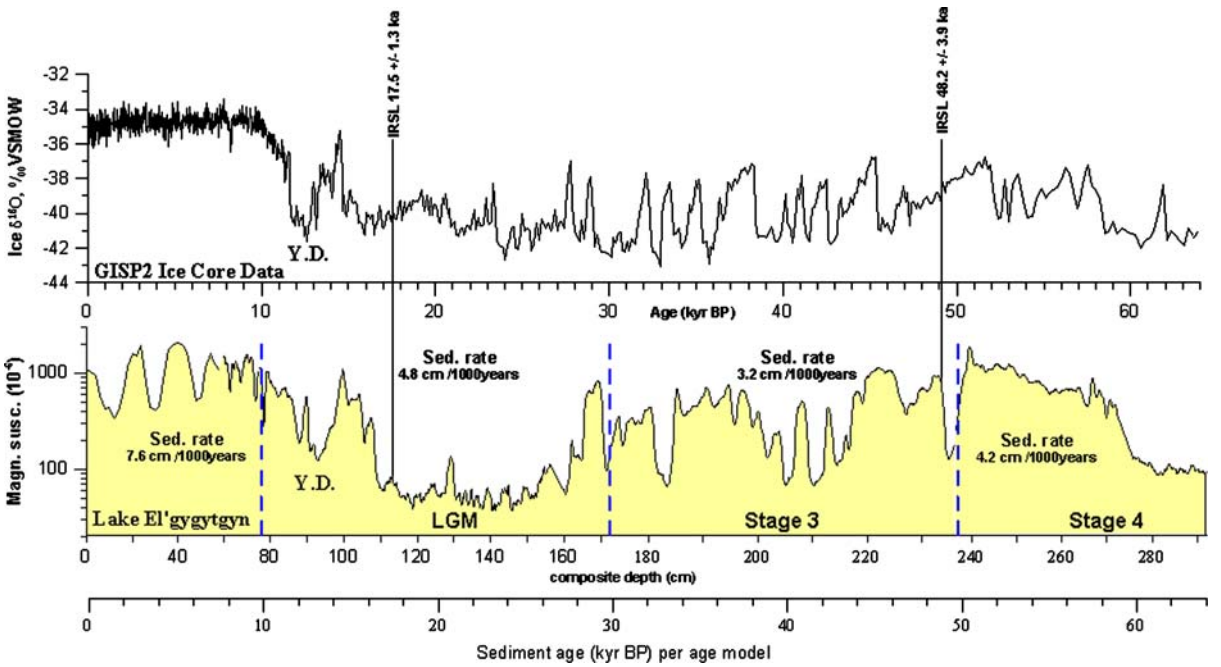

Fig. 3 The magnetic susceptibility of the upper 300 cm of the cores from Lake El'gygytgyn is tuned against the $\partial^{18}O$ from the GISP2 record (Grootes et al. 1993; Nowaczyk et al. 2007). IRSL ages calculated for the core has been added as additional chronology controls. The depth scale of the magnetic record is shown with sediment age given below. Sedimentations rates were calculated for the existing age model (Nowaczyk et al. 2007). Based on this chronology, a sedimentation rate of 7.6 cm/1,000 years is calculated for the Holocene, 4.8 cm/1,000 years during the LGM, 3.2 cm/1,000 years in MIS3, and 4.2 cm/1,000 years for MIS4

10 m and are coved with sand to cobble sized stones, which in some locations form beach berms that can be ≤4 m high. Following the spring snow melt, in early to mid-July, loose pans of ice are shoved onto the beaches by strong winds. These ice-shove events ramp up into the beach deposits, increasing the size of the beach berms. The berms are also maintained through much of the summer season by wave action during storm events. Furthermore, spring melt dramatically increases erosion processes from the lake watershed (Nolan and Brigham-Grette 2007). These small, low energy inlet streams increase in flow and carry pebble to cobble-size rock and clumps of tundra, which are deposited on the lake shelves and beach (Fig. 4). The melt season is dramatic but short lived, and the inlets quickly return to a low-energy state. Following the melt season, few streams can break through the berm deposits, allowing the berms to act as an effective filter to further transport of coarse sediment into the open lake.

In 2000, as in most years, the hydrologic input from these streams decreased dramatically over the summer. Lake level measurements decreased approximately 1 m from August until the beginning of September. Additionally it was determined that the lake lacked a thermocline or chemocline. Rather, the water temperature (~3°C), pH, and O_2 were nearly constant throughout the vertical water column (Nolan and Brigham-Grette 2007). Today, the lake is ice-covered nine to ten months each year, with open water from mid-July to mid-September.

Seismic lines collected in summer 2000 showed that the lake basin is filled with over 360 m of sediment overlying a brecciated crater floor with an ill-defined central dome (Niessen et al. 2007). Debris flow lenses where discovered in the initial study, but do not extent to core PG1351. However, we now have evidence that minor graded layers, presumably settled from the suspension clouds produced by debris flows, do extent to this core and are expressed in the grain-size data as

Fig. 4 Photo taken during the 2000 field season; stream #12 (Nolan and Brigham-Grette 2007) along the western shore of the lake showing the storm berms which filter the stream sediment load as it enters the lake basin

''non-erosive'' event layers (Olaf Juschus, pers. commun. 2005).

Methods

Sample collection and preparation

The sediment core PG1351 was collected through lake ice, using a percussion piston corer suspended on a 4 m tripod (Melles et al. 2007). The core was cut into 1-m segments and transported unfrozen to the Alfred Wegner Institute-Potsdam (AWI), Germany for sub sampling. The cores were split into two halves; one half was described for physical stratigraphy and photographed and the second was archived at AWI for future study. The working core was then sub-sampled in 2 cm intervals; samples were weighed before and after freeze-drying for water content, split into sixths, and transported to the various scientific partners for analyses. Nearly 650 samples were separated and logged for analyses of clay mineralogy and grain-size at the University of Massachusetts.

Core description

The core cycles between well-laminated to non-laminated (or massive) lacustrine mud sequences (Fig. 5). Thin-sections prepared for this core illustrate this change. The lithology is dominated by clayey-silt, silty-sand horizons and several intervals containing diatomaceous sediment. The color range is gray to very dark gray (Munsell Colors, 5Y: 5/1, 6/1, 3/1, 4/1; 2.5Y: 4/1, 5/1, 6/1), to shades of olive gray (Munsell Colors, 5Y: 3/2, 4/2, 4/4, 5/2), and gray-brown (Munsell Colors, 2.5Y 4/2, 5/2). A compilation of these colors has been done for the upper 300 cm.

To document the occurrence of the laminated versus non-laminated units, a semi-quantitative bioturbation index (Behl and Kennet 1996) was estimated for the full 1,300 cm core using photos and physical core descriptions. Each 1 cm interval was assigned a value from 1 to 4 with 1 defined as well-laminated and 4 as non-laminated or massive. Identification of the laminae between 1 and 4 is subjective; therefore the index was calculated three times. Comparison of the three calculations showed them to be reproducible within 5%. Further, thin-sections from the soft sediment were prepared for a microscopic view of the laminated versus non-laminated units (Francus and Asikainen 2001).

The mineral vivianite appears in the core as either millimetric-size granular crusts or as highly fissile nodules that range in size from 1 to 8 mm. Vivianite is a reduced iron phosphate $Fe_3(PO_4)_2{-}(H_2O)_8$ and was identified using petrographic and quantitative microprobe analyses. Vivianite occurs most frequently within the laminated sequences and varies in concentration throughout the core.

A distinctive feature in the core is the occurrence of relatively large spherical to elongate clusters (interclast) of grains that range in size from ~1 mm to a little over 1 cm in diameter that are not well described in the literature. These structures contain a variety of rock fragments that are angular to well-rounded in shape and occur

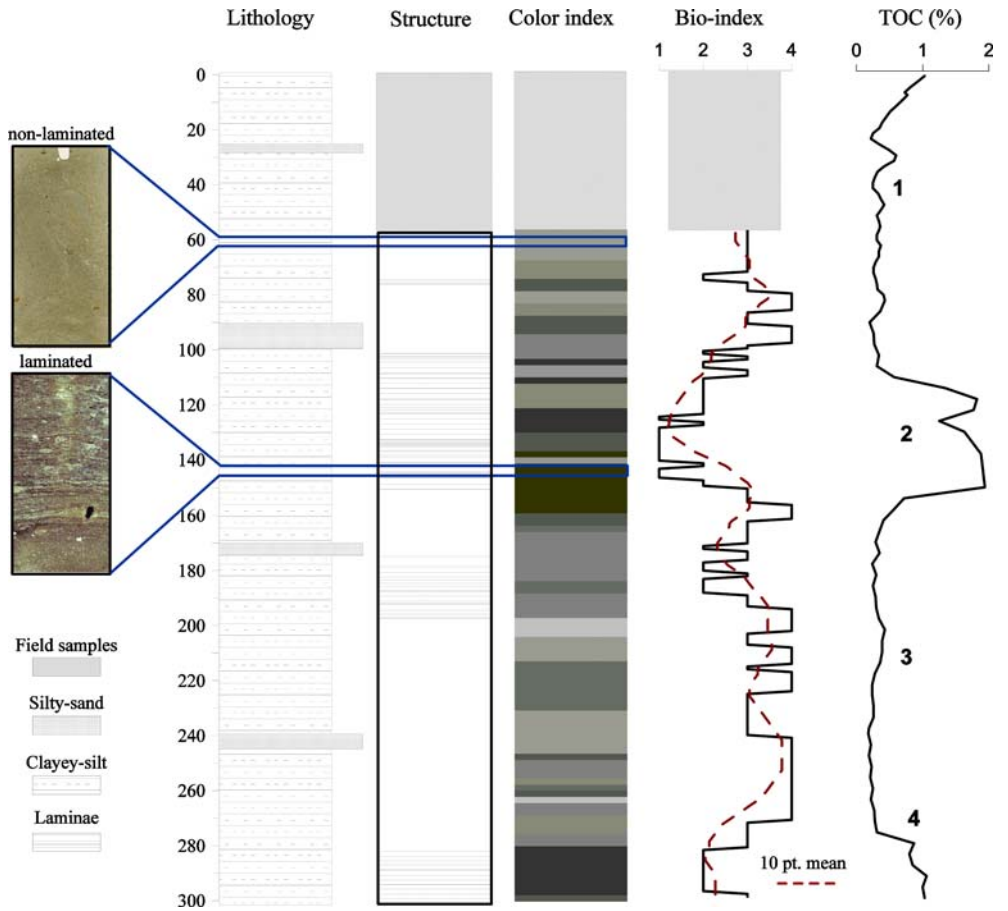

Fig. 5 The description of the core lithology is plotted with the structure, relative color changes, bioturbation index and TOC percent from Melles et al. (2007). The laminated and non-laminated units are dominated by clayey-silt and are distinguished only by the preservation of laminae. Units that contain silty-sand do not occur in the laminated units. Petrographic thin-section photographs show the visible differences between non-laminated (top) sediments (60–62 cm) and laminated (bottom) sediments (143–145 cm). A bioturbation index was developed using a score of 1 for well laminated intervals and 4 for non-laminated intervals after Behl and Kennett (1996), is plotted with percent TOC percent from Melles et al. (2007) show that preservation of laminations (both with and without a 10-point running mean) coincide with periods of high TOC. Marine isotope stages 1–4 are indicated on the TOC graph are inferred from the correlation of magnetic susceptibility and $\delta^{18}O$ from the GISP2 (Fig. 3)

throughout the core but are most common in the laminated segments where no bioturbation of the sediment is found. Because these interclasts do not account for a significant portion of the material in the core, they have little effect on the grain-size analyses. Preliminary results using scanning electron microscopy show the structures to differ in grain-size and sediment structure from the surrounding sediment. The exact origin is unclear but may originate from ice-rafted debris, frozen mud balls, or post-depositional compaction.

Clay mineral analyses

Clay minerals were analyzed from cores PG1351 using a standard method (Yuretich et al. 1999). Approximately 5 g of freeze-dried sample was crushed with a mortar and pestle and disaggregated in deionized water (DI) using an ultrasonic dismembrator. The clay size (~2 μm) fractions were separated by centrifugation. Oriented samples were produced by spreading the separated clay fractions onto a petrographic microscope slide (Yuretich et al. 1999).

The air-dried samples were scanned from 2 to 32° at a step rate of 0.05° 2θ for base peak identification data using a Philips X-ray diffractometer (XRD) with a 1.541874 Å Cu$K\alpha$ radiation (Fig. 6a). Ethylene glycol-solvation was performed on each sample (8 h at 60°C) to test for the presence of expandable-layer clays such as smectite, typically represented by a shift in peak position and intensity (Moore and Reynolds 1989). Additional treatment with a 1 molar (M) magnesium (Mg) solution was performed on 20 samples to distinguish between clay species of smectite and vermiculite (Moore and Reynolds 1989). Twelve samples that exhibited XRD patterns with a low shoulder peak at 7 Å were tested for the presence of kaolinite by heating to 550°C

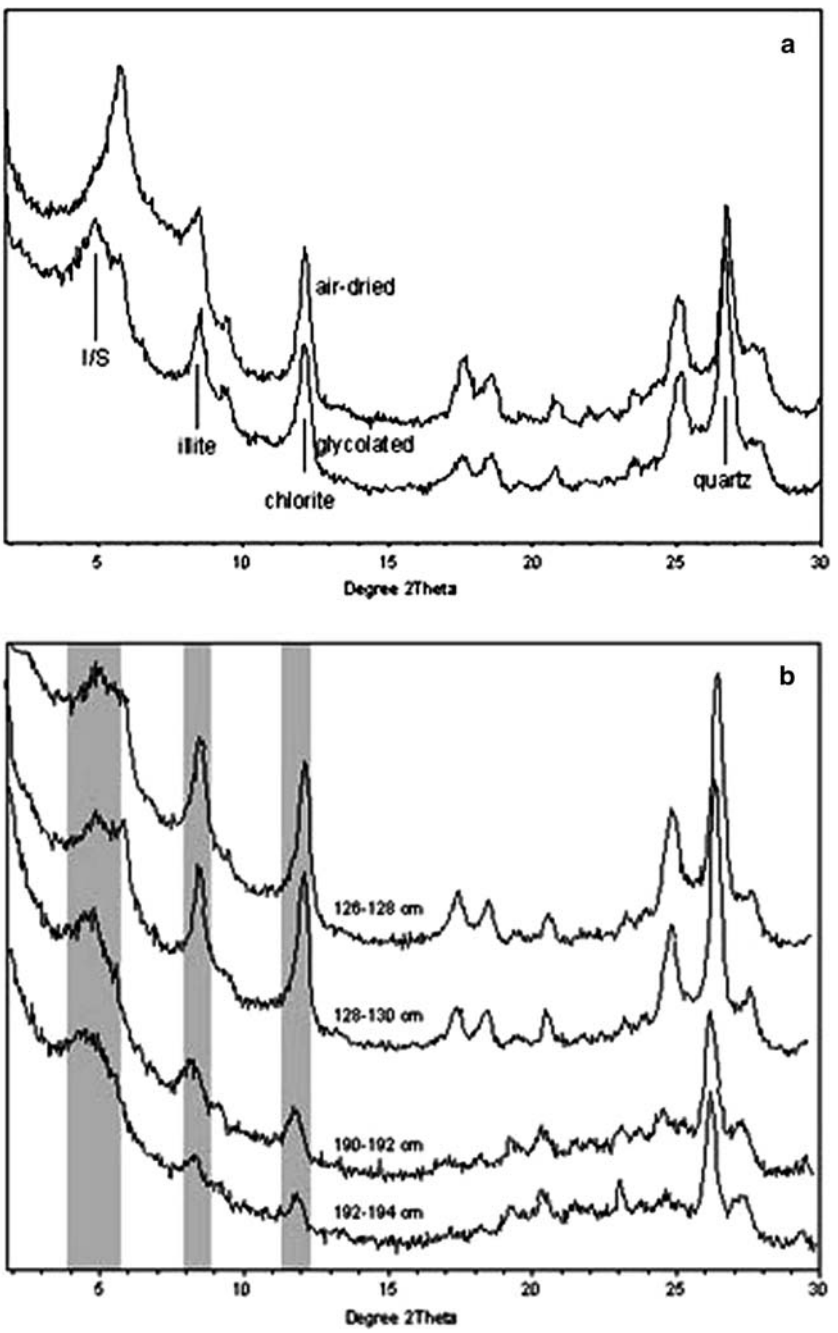

Fig. 6 X-ray diffractograms from representative samples. (**a**) Shows air-dried (upper) and glycolated (lower) treated samples from 109 cm depth. The clay minerals identified are smectite, illite, chlorite and highly interstratified illite/smectite. Note that the first peak at 6° 2θ in the air-dried spectrum shifts to 5.2° 2θ with a low shoulder pattern, which is consistent with highly interstratified illite-smectite (*I*/*S* + *Sm*); (**b**) Comparison of X-ray diffractograms from composite depths with high chlorite (126–130 cm) and low chlorite (190–194 cm)

for 1 h (Moore and Reynolds 1989). Following each treatment, an XRD pattern was collected for each sample.

The minerals were identified by reflection peak analyses of glycol-solvated samples using the MacDiff Program version 3.1 (Petschick et al. 1996; Fig. 6b). Relative percentages calculated from MacDiff integrated peak area intensities (identified by MacDiff as F[Σ]) are estimated from *d*-spacing of: 15 Å, expanding to 17 Å on glycol treatment for smectite; 10, 5, and 3.333 Å for illite; and 14.2, 7.1, 4.74, and 3.55 Å for chlorite.

Relative percentages calculated here are based on the approximate 17 Å peak for illite/smectite and the 7.1 Å peak for chlorite. When non-crystalline matter is present and the peak areas are normalized to 100%, the results suffer from the closure problem (Moore and Reynolds 1989). In an attempt to solve this issue, we applied the Biscaye formula (1964) however it yielded no significant change.

Using the MacDiff program, crystallinity was measured on the illite 10 Å peak (Fig. 6b). Crystallinity is defined as the Full-Width Half-Maximum and is a measurement of the width of the curve at half the height and is inversely proportional to the crystallinity of the illite clay mineral (Petschick et al. 1996). The smaller the half-width measurement, the more ordered or well crystallized the mineral (Chamley 1989).

Grain-size analyses

Organics, biogenic silica, and vivianite crystals were removed from the sample to exclude any features not directly related to clastic sedimentation. Approximately 2 ml of sample was placed into a 15 ml centrifuge vial. Organic matter was removed by adding about 10 ml of a 30% hydrogen peroxide (H_2O_2) solution to each vial, heated in a 50°C water bath overnight, and rinsed with DI to remove excess H_2O_2. A 1 M solution of sodium hydroxide (NaOH) was prepared to remove biogenic silica. Each sample was placed in a 50°C bath for 4 h, shaken for 30 min in a recapitulating table, then returned to the water bath for 1 h, and subsequently rinsed with DI H_2O to neutralize NaOH.

No standard method was available to dissolve the vivianite crystals from the sediment. We developed a method by using solubility curve data to determine the minimum strength of nitric acid (HNO_3) needed to dissolve the crystals. We determined that a 0.5 M solution of HNO_3 was sufficient for complete dissolution of vivianite, following the same heated water bath and shaker regiment used to remove the biogenic material above (Al-Borno and Tomson 1994; Malo 1997). Smear slides were inspected under a petrographic microscope to confirm that all crystals had been removed.

After the final centrifuge, excess liquid was removed using a Pasteur pipette. Samples were dried to a paste for measurement on the Coulter Ls 200 (CL200) laser particle analyzer. This instrument measures the volume percent of selected bin-size ranges in a sample from 0.488 to 2,000 μm (Sutinen et al. 1993). To avoid flocculation during the measurement of the particle, a sodium metaphosphate solution was added to the sample and was than sonicated for 60 s. Each sample was run for three cycles because it was determined that the particle size distribution remained constant after the third cycle. Replicate samples, at intervals of 20 cm, showed that the general patterns in grain-size distribution are consistent and repeatable. We tested the newly developed method on a set of 12 samples. The removal of authigenic material produced as much as a 10% shift towards finer size in the volume percentages of the grain-size distribution. Because the abundance of vivianite is highly variable throughout the core, this treatment was applied to all samples. The geochemical proxies (TOC and Biogenic silica) used for comparison in this paper are discussed in Melles et al. (2007).

Results

Bioturbation and sedimentation

The bioturbation indexe is in phase with magnetic susceptibility (Fig. 2). This on–off pattern in laminations is easily seen in the upper 300 cm of the core during MIS 2 and 4 (Fig. 5). In this upper interval, high bioturbation indices coincide with

low TOC values, especially during marine isotope stage 1 and 3 (Fig. 5).

Sedimentation rate was calculated for the LGM and Holocene yielding 4.8 cm/1,000 years and 7.6 cm/1,000 years, respectively. Sedimentation rate was calculated using the current age model proposed by Nowaczyk et al. (2007).

Clay results

A shift of the 6° 2θ (15 Å) 001 diffraction peak (Fig. 6a) to 5.2° 2θ (16.9 Å) induced by the ethylene glycol-solvation confirmed the presence of smectite (Moore and Reynolds 1989). Further, these glycol-solvated samples showed that the 15 Å diffraction peaks are broad with a high low-angle shoulder pointing to a mixed layer smectite species interstratified with illite (Moore and Reynolds 1989; Fig. 6a, b). The location and shape of the 16.9 Å peak on the treated samples suggests disordered layers or a random interstratification rich in smectite (Moore and Reynolds 1989; Fig. 6a).

The 16.9 Å peak of glycerol-solvation samples remained unchanged after Mg treatment, confirming smectite development over vermiculite (Moore and Reynolds 1989). Kaolinite is not present in the 12 heated samples, as no reduction in the peak intensity was found (Moore and Reynolds 1989).

The Reichweite method (ordering of mixed-layered clays) was used to determine the percentage of illite in the *I*/*S* interstratified clay species. The Reichweite method or *R*-value, expresses a terminology for the probability that one clay species will follow the second clay species (Moore and Reynolds 1989). Examination of the 16.9 Å peak of ethylene glycol-solvated samples shows a strong broad reflection, which is consistent with a random nature mixed-layered clay *I*/*S*. The illite to smectite percentage is difficult to determine because reflection is not well developed or is obscured by other clays on the XRD diffractogram. Ordering of the layers is present when the illite to smectite ratio is >50% (Moore and Reynolds 1989). Because no ordering is seen, it is reasonable to estimate the ratio to be 50% or less illite. Based on the peak to valley ratio of the illite to smectite, smectite may represent 80–90% of the mixed layer clay (Moore and Reynolds 1989).

The clay mineral assemblages range from 5% to 20% chlorite, 23% to 38% illite, and 40% to 70% smectite, and highly interstratified illite + illite-smectite (*I*/*S* + *Sm*). In Fig. 7 relative abundances were plotted for percent interstratified *I*/*S* + *Sm* and chlorite. Illite was not plotted independently as it represents a relatively stable fraction of the total *I*/*S* + *Sm*. As an example of the variability in the chlorite clay species throughout the core, we display the diffraction patterns for high chlorite from 126 to 130 cm and from 190–194 cm patterns (fig. 6b).

As indicated above, the clay mineralogy is dominated by interstratified *I*/*S* + *Sm*. Chlorite shows an inverse correlation to *I*/*S* + *Sm* downcore, even though the relative abundance is lower (Fig. 7). The data shows four significant shifts in relative abundances versus depth that are concurrent with shifts in magnetic susceptibility of core PG-1351. Based on clay percentages (below or above 50% *I*/*S* + *Sm* in the smoothed curve), we defined four time intervals labeled A–D in Fig. 7. More subtle shifts underline the variability within specific intervals. In intervals A and C (0–80 cm and 165–225 cm; Fig. 7), *I*/*S* + *Sm* clay minerals range between 50% and 70%. Chlorite in this portion of the record stays between 5% and 15%. Intervals B and D (80–165 and 225–300 cm) show a 15% increase in chlorite percent (15–25%) with a corresponding 15% decrease (38–50%) in *I*/*S* + *Sm* abundance. Correspondingly, the crystallinity of the illite shows a similar pattern throughout the core. Clay and illite crystallinity data is shown with a 5-point running mean curve (Fig. 7).

Grain-size results

Grain-size of sediments in Lake El'gygytgyn are plotted in non-cumulative volume percent for 230 samples with size fractions separated into clay (<2 μm), silt (>2 μm to <62.5 μm), and sand (>62.5 μm) (Fig. 8). The lake sediments are fine grained, with few grains exceeding 65 μm. The mean and the median grain-size are 6.92 and 4.07 μm, respectively; all within the fine silt-size fraction. In fact, 98% of total volume percent is

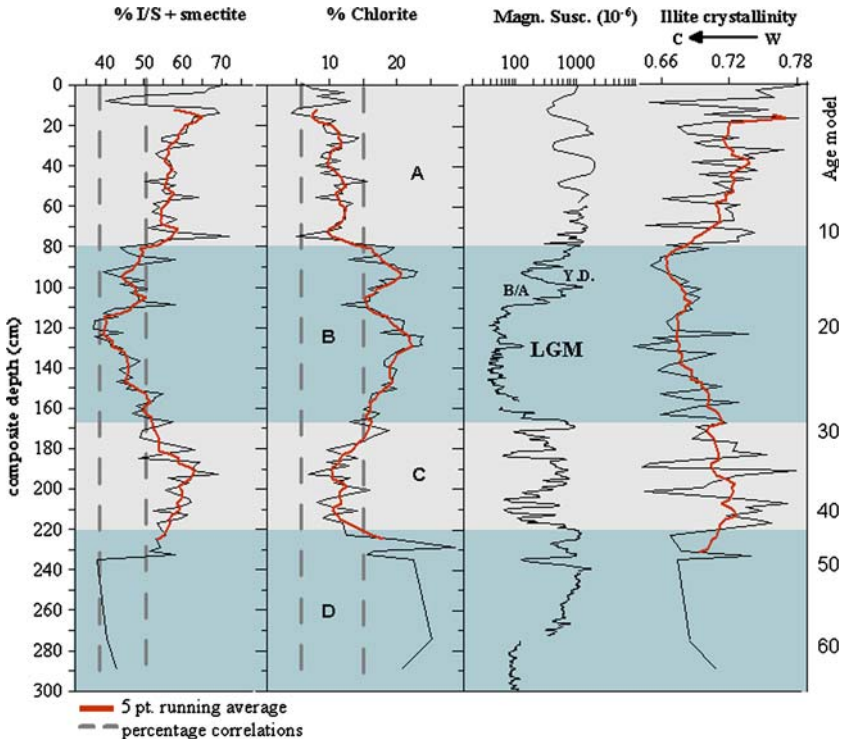

Fig. 7 Relative clay abundances, illite crystallinity are plotted with magnetic susceptibility showing the inverse relationship between chlorite and illite/smectite. Shaded areas outline four intervals that are distinguished by changes in clay mineral abundance and roughly coincide with the MIS 1–4 from Fig. 3. Intervals A and C, are characterized by $I/S + Sm$ in the range of 50–70%, suggesting warmer conditions. Intervals B and D suggest cooler conditions as indicated by higher content in chlorite (15–25%). The vertical dashed gray lines outline consistent percent changes in clay abundances as outlines above. Directly above the LGM shifts in magnetic susceptibility indicate a pronounced warming (increase in magnetic susceptibility), followed by a pronounced cooling event (decrease in magnetic susceptibility), that is seen in the clay percentages, and to some extent, in illite crystallinity. Based on the current age model (Nowaczyk et al. 2007) these shifts in magnetic susceptibility and clay characteristics can be correlated to warm episode of the Bolling/Allerod (B/A) and cold episode of the Younger Dryas (Y.D.) respectively. LGM is Last Glacial Maximum

silt-size or less with only 2% of the samples in the sand size fraction and are expressed in the grain-size data as ''non-erosive'' turbidity flows (Olaf Juschus pers. commun.). The clay-size fraction is 51% and the silt-size fraction is 47%. Most of the measured samples exhibit a complete lack of tailing versus larger grains (Fig. 8, GSD1 and GSD3). Additionally, the distribution of the fine grained material shows distinct bi- and tri-modal patterns in the clay and silt sized fractions. A normal tailing of larger sediment was observed only in samples with grain-sizes exceeding 100 μm (Fig. 8, GSD2).

Three main grain-size distribution (GSD) patterns emerge from the analysis, each occurring preferentially within distinct intervals and referred to here as GSD1, GSD2, and GSD3 (Fig. 8). In the upper interval, the GSD1 pattern of sedimentation is tri-modal (particle size mode 2.5 μm) with a relatively broad peak in the silt-size particles and no tailing (Fig. 8). The particle size mode in GSD3 is roughly the same as in GSD1 (Fig. 8), however it contains slightly more clay size particles, and the silt peak is lower (~20–50 μm). The GSD2 particle size mode is 31.5 μm with a tailing that extends to 250 μm (Fig. 8) and the clay fraction is greatly reduced but the silt size fraction remains high.

The down-core grain-size distribution is shown in separated grain-size fractions along with magnetic susceptibility and the isotopic stages in Fig. 8. The clay, silt, and sand fractions show

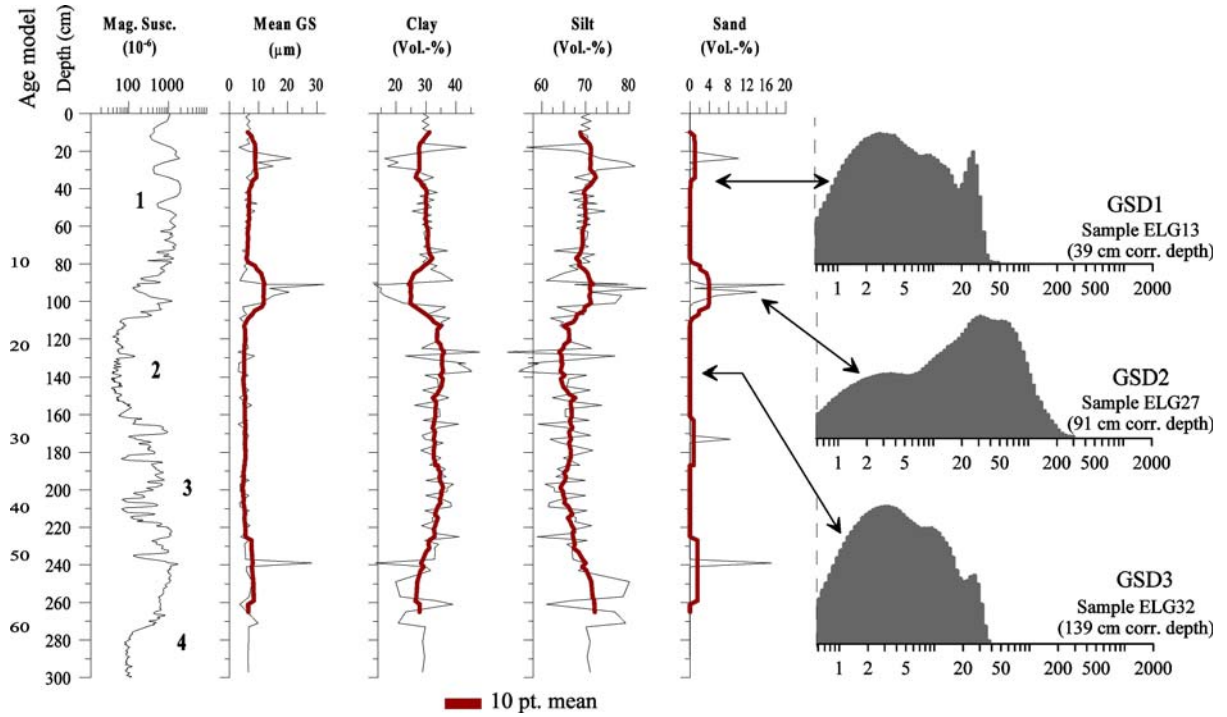

Fig. 8 Volume percents grain-sizes in the clay-size fraction, silt-size fraction, and sand-size fraction are plotted with mean grain-size and magnetic susceptibility. As a reference MIS1–4 and Nowaczyk's 2007 age model have been added. Three representative grain-size distributions shown in microns are GSD1, GSD2, and GSD3. GSD1, this tri-model pattern is common during warmer climate conditions, GSD2, this distribution pattern shows tailing of grain-size which only appears in samples with grains larger then 100 μm, and GSD3, a pattern interpreted as cooler periods when the silt fraction between 20 and 50 μm is less important compared to GSD1

noticeable shifts in volume percent between 23–28, 89.5–100 and 239–241 cm. Mean grain-size (shown in actual grain-size not volume percent) has little variation as the predominant grain-size is within the silt fraction. Because they contribute equally to the overall size fraction, the fluctuations of the clay and silt fractions are in anti-phase.

Discussion

Sedimentary units

The laminated intervals in the core correspond approximately to intervals with low magnetic susceptibility whereas massive intervals correspond to intervals with high magnetic susceptibility values (Fig. 2) as seen in the semi-quantitative bioturbation index. Further, the index shows that non-laminated intervals coincide with warmer interglacial periods and laminated intervals occur during glacial periods (Figs. 2, 5). We interpret these changes in sedimentary units as an indicator of available oxygen in the hypolimnion during glacial/non-glacial periods and the lack of mixing in the water column. During glacial periods, the ice cover on the lake is thought to become permanent or semi-permanent, reducing the exchange between atmospheric oxygen and lake water and reducing wind activity (Wetzel 1983). The benthos mixing at the sediment/water interface that disturbs the primary sedimentary structure cannot survive in these oxygen poor environments. Further, much of the anoxic environment in lakes occurs up to 20 cm below the sediment/water interface (Nealson 1997) and changes oxygen levels are a function of the amount organic carbon that reaches the sediment. When the sediment is undisturbed, due to ice

cover, sediments will become anoxic (Nealson 1997).

Anoxia is interpreted to cause dissolution of the magnetic grains and is therefore responsible for the low magnetic susceptibility values during glacial intervals (Nowaczyk et al. 2002). This interpretation is further supported by the frequent occurrence of vivianite in laminated units (Al-Borno and Tomson 1994; Fig. 2). This diagenetic mineral is common to lacustrine sediments worldwide in reducing redox environments (Al-Borno and Tomson 1994; Mothersill 1996). The lack of mixing in the sediments limits the availability of oxygen, which sets up the potential for a chemical gradient that results in anoxic sediments (Nealson 1997; Mothersill 1996). Vivianite production is stable in reduced conditions (pH 7–12) which is well within the range observed in Lake El'gygytgyn (Nriagu and Dell 1974).

The formation and preservation of laminations may be due to factors other than variations in the oxygen content of the water column (Francus 2001). The occurrence of laminations is unlikely to be the result of an increase in sedimentation rate since, according to the age model, sedimentation is 4.8 cm/1000 years during glacial periods (Nowaczyk et al. 2007; Fig. 3). It is reasonable to infer that during glacial times, sediment availability in the watershed is reduced due to the lack of or an extremely thin active layer over the permafrost in the catchments. Sediment delivery also may have been reduced by the presence of a closed ice cover on the lake as measured in the perennial ice-covered lakes of Antarctica (Priscu et al. 1998). Finally, another possibility is that the presence or absence of lamination might be due to the presence or absence of seasonality in the sedimentary input. If so, then seasonality and hence the formation of laminations should be strongest during interglacial periods, i.e. with the occurrence of a well marked melting season, compared to the permanently frozen landscape during glacial periods. Because laminations are observed during glacial intervals, we reject this later explanation.

In Fig. 5 total organic carbon (TOC) is plotted with bioturbation index and core lithology (Melles et al. 2007). During the LGM, between 100 and 170 cm there is a decrease in magnetic susceptibility, an increase in TOC percent, yet biogenic silica remains nearly constant (Melles et al. 2007). This apparent discontinuity has been interpreted by Brigham-Grette et al. (2007) as an indication of the cold/dry or windy climate conditions that prevailed in this region during the LGM. Under perennial ice-cover, anoxic conditions in the deepest part of the lake preserve organic matter from decomposition (Vigliotti et al. 1999). Additionally, snow-free ice allows solar irradiance to support a diatom community under the ice (Andersen et al. 1993; Mackay et al. 2000), maintaining productivity and therefore the supply of organic matter to the hypolimnion.

As shown in Fig. 5 the color change in the core to dark gray is coincident with changes in the bioturbation index, magnetic susceptibility and TOC during the LGM and marine isotope stage 4. The change in sediment color can be interpreted as a change in oxygen levels due to the reduction of iron within the sediment during periods of perennial ice cover (Nowaczyk et al. 2002).

Clay mineralogy

Four time intervals can be distinguished based on changes in clay mineral abundance (Fig. 7). Intervals A and C, are characterized by $I/S + Sm$ in the range of 50–70%, suggesting warmer, more hydrolyzing conditions. In the same intervals chlorite is between 5% and 15% presumably reflecting persistent weathering. Intervals B and D suggest cooler, dryer conditions as shown by a 10% higher content in chlorite (15–25%) and a 18% lower abundance (38–50%) in illite/smectite.

Putting these intervals into the chronological framework established by the magnetic susceptibility (Nowaczyk et al. 2007), the following climate succession was reconstructed. Directly above the LGM, magnetic susceptibility shows a distinctive shift to warmer then back to cooler conditions coincident with shifts in clay mineral abundance changes. According to our chronology this transition occurs between 11.6 and 14.5 ka, placing it between the Younger Dryas cooling period and the warmer Bolling/Allerod (Fig. 7; Grootes et al. 1993). The Younger Dryas cooling event is also evident at about 95 cm (composite

depth), coinciding with the GISP2 record at ~12 ka (Figs. 3, 7).

Clay minerals are formed in the soils of the tundra surrounding Lake El'gygytgyn. These minerals are eroded and then carried over time into the lake basin by the many inlet streams. The change in percentage between chlorite and *I/S + Sm* reflects the availability of these minerals to the system. Because chlorite represents unweathered clay species, it is readily available for transport into the system. In contrast *I/S + Sm* represent the weathering product of chlorite and would only be available for transport during warmer interglacials when thickening of the active layer increases the accessibility. Further, Blaise (1989) has shown that this predictable progression of clay minerals from chlorite through illite and smectite is related to changes in climate conditions from cold and dry to warm and moist. For example, smectite formation, which in the core interstratifies with illite, is influenced by chemical weathering and thus is an indicator of warm and wet climate conditions (Berner 1971; Chamley 1989). In contrast, higher relative abundance of chlorite indicates a dryer cold climate prevailed, preserving chlorite that is otherwise highly susceptible to weathering in moist hydrolyzing conditions. The abrupt decrease in magnetic susceptibility at 160 cm is accompanied by a gradual increase in chlorite over a 30 cm interval, which reaches the greatest abundance at 120 cm. The clay minerals in this core demonstrate that relative changes in clay mineral abundance record climate induced changes in the catchment. The high chlorite to smectite formation can be seen in the XRD diffraction patterns in Fig. 6b. Despite its high latitude, El'gygytgyn sediment cores show a distinct downcore inverse relationship between *I/S + Sm* and chlorite clay species (Fig. 7), supporting the hypothesis that changing weathering conditions are being recorded in the watershed due to climate fluctuations.

The transformation, rather than total neoformation of a clay mineral from well crystallized to poorly crystallized also coincides broadly with changes in climatic conditions (Chamley 1989). Crystallinity is not preserved under warm hydrolyzing conditions because it initiates an increased cation substitution within the clay structure, which distorts the crystal lattice. The illite crystallinity curve follows this trend showing synchronous intervals with magnetic susceptibility and the relative clay abundances (Fig. 7). Within the crystallinity data, the largest shift occurs at ~78 cm which is coincident with the end of marine isotope stage 2, supporting the general trend we seen in the magnetic susceptibility from cooler to warmer climate conditions in the late Holocene.

Grain-size distribution

Magnetic susceptibility is a measure of magnetic mineralogy and is widely used as a proxy for variations in lithostratigraphy (Peck et al. 1994). In most other studies, grain-size distribution has a direct relationship to magnetic susceptibility because the carrier mineral that retains the remnant magnetic intensity has a specific grain-size distribution and reflects a particular particle size (Vigliotti et al. 1999).

This study confirms that the magnetic susceptibility signal in Lake El'gygytgyn is largely a function of dissolution and not grain size or organic content (Fig. 5; Nowaczyk et al. 2002). Despite the difference in sampling resolution (grain-size every 2 cm, magnetic susceptibility averaged every 1 mm), Fig. 8, in particular, clearly shows that the grain size data, especially mean grain size weighted by silt, are rather monotonous. This is true in spite of changes in magnetic susceptibility of nearly two orders of magnitude throughout the record. Even the increase in fine sand at about 97 cm is associated with a increase in magnetic susceptibility, rather than an decrease as one might expect of materials derived from highly susceptible rocks. However, the grain-size data show interesting characteristics when examined in detail. For example, several of the shifts seen in the sediment fabric (Fig. 5) and clay mineralogy are present in the grain-size distribution analyses from Lake El'gygytgyn (Fig. 8).

The poly-modal character of the GSD patterns (Fig. 8) suggest multiple modes of transport into the deepest parts of the lake (Last 2001). The GSD1 pattern is coincident with the generally warmer climate of the Holocene (Fig. 8). During these warmer intervals, the sedimentation is due

to fine hemipelagic settling. We believe that the absence of a tail is due to the filtering effect of the storm berms along the shores through which the tributaries need to flow. The silt peak at 20 μm is likely due to some additional aeolian input from the surrounding catchment and resuspension of fine material during summer storms. Additionally, several inlet streams have been observed to transport sediment onto the ice cover (Brigham-Grette, pers. commun. 2004; Vologina et al. 2003). This phenomenon may also account for the incorporation of coarser sediment onto the lake ice in the littoral zone and its supply to the more distal parts of the lake during melting of the ice cover (Vologina et al. 2005).

The GSD3 type is largely dominated by the clay fraction and is due to sedimentation under perennial ice (Fig. 8). Indeed, in such situations sediment can make its way only through small cracks in the ice cover or via the seasonal moat that's surrounds most of perennial ice covered lakes in summer. Sediment supply may be influenced by regional eolian transport that falls onto the ice cover and moves through the ice cover. Sorting effects of this mode of sedimentation would explain the relative decrease of the larger silt fraction peak seen in GSD1. Moreover, the ice cover reduces the possibility for water currents strong enough to transport coarse grained sediments to the center of the lake, allowing only particles in suspension to settle in the pelagic zone. These mechanisms might explain why so little coarse silt makes its way to the center of the lake. Sedimentation trap data will be needed to resolve this problem.

The GSD2 pattern has the coarsest grain-size mode, although just as seen in GSD1 and 3, the silt and clay fractions still dominate (Fig. 8). We interpret this GSD2 pattern to be the result of both pelagic settling and possibly to a ''non-erosive'' debris flow elsewhere in the basin. Deposits resulting from ''non-erosive'' debris flows were identified in cores collected in 2003 from a slightly more proximal location compared to PG1351. Non-erosive debris flows resulting from the settling of distal particles from suspension clouds following Stokes Law produce graded layers which can have larger grain-size at the base. Debris flows in the 2003 core are thin but varied in thickness. Based on stratigraphic correlation, they occur at 22–28, 89.5–100 and 128–129.5 cm (Olaf Juschus pers. commun. 2005) when transposed on the PG1351 composite depth. The debris flow between 22–28 cm and 89.5–100 cm are supported by our record (Fig. 8). However, the absence of an increased grain-size at 128–129.5 and the presence of sand sized peaks at 170–172 and 238–241 cm, tasks us to explain this lack of correlation. The 2 cm sampling resolution of this core may explain the absence of the 128–129.5 cm interval because each sample may have contained only a portion of this 1.5 cm debris flow, thus reducing the amount of larger grain-sizes in each sample. Alternatively, there may have simply not been enough energy in this small debris flow to blanket the entire lake bottom. More disturbing is the presence of sand-size peaks at 170–172 cm and 238–241 cm, not present in the Juschus debris flow study. However, the increased grain-size peaks occur in middle and at the end of marine isotope stage 3, which may indicate a time of increased precipitation coincident with the thawing of the active layer across the tundra, likely provided more sediment available for transport into the lake.

Anderson and Lozhkin (2002) have recently compiled much of what is known concerning the paleoclimate records from lakes throughout Chukokta. It is clear from their review and regional synthesis of the paleoenvironmental records of the past 65 ka that spans most of western Berinia (Brigham-Grette et al. 2004; Anderson et al. 2004) that only a handful of lakes have records extend beyond 60 ka (Anderson and Lozkin 2002). Furthermore, most of these records focus on the palynology and vegetation history of the region and do not include sedimentology and clay mineralogy. We believe that the work presented in this paper on Lake El'gygytgyn is the first of its kind in Chukotka.

The sedimentological data from El'gygytgyn Lake shows that the climate of western Beringia was rather variable and unstable throughout MIS 3 reminiscent of the changes in vegetation recorded at Elikchan 4 Lake (Lozkin and Anderson 1996). Although the pollen record of this same time period in Lake El'gygytgyn lacks these dramatic shifts (Lozhkin et al. 2007), changes in regional

temperature must have been of sufficient amplitude to influence the duration of summer lake ice cover and, in turn, shift the geochemistry of the lake to influence magnetic mineral dissolution and preservation via intervals of summer anoxic and oxic conditions. Our data would suggest that similar shifts may have also occurred in the precipitation and snow cover, two variables that would have had a direct influence on clastic input and rates of weathering. Although we lack the sampling resolution and age control to make any plausible correlations between our record and that of Elikchan 4 Lake, both records share the characteristic variability we have learned to expect from global records for this time period (30–65 ka), like those seen in the Greenland Ice sheet record (Fig. 3).

Similarities with the Greenland record are also found in the LGM and deglacial portions of records from western Beringia. Given the constraints on the geochronology (Brigham-Grette et al. 2007; Forman et al. 2007), it was Nowaczyk et al. (2002) who first suggested that the drop in magnetic susceptibility at 97 cm was likely correlative with Younger Dryas cooling. This drop in susceptibility is coincident in our data with a shift to higher percentages of chlorite as seen during the LGM. Records of a Younger Dryas cooling are continuing to emerge from records throughout Beringia, most recently from Smorodinovoye Lake west of El'gygytgyn in the upper Indigirka Basin (Anderson and Lozkin 2002), and Grandfather Lake in SW Alaska (Hu and Shemesh 2003), a lake not far from moraines of Younger Dryas age in the Aklun Mountains.

Conclusion

The variability in sedimentology, i.e. clay mineralogy, bioturbation, and modes of sedimentation in core PG1351 from Lake El'gygytgyn confirm distinguishable intervals in sediment characteristics in the upper 300 cm. These intervals (A–D in clay mineralogy) are coincident with the glacial-interglacial cycles, thus MIS 1–4 during the last 65 ka (Fig. 7).

The most important factors affecting the sedimentology in Lake El'gygytgyn are the duration of perennial ice-cover and the thickness of the tundra active layer. During warm periods (interval A and C; Fig. 7) the lake is ice-free most of the summer. This climate pattern is marked by massive or non-laminated sediments, an increase in $I + IS$ clay mineral, and (for the most part) higher sedimentation rates. Melting of the ice cover during the summer months provides oxygen to the entire water column, which supports the presence of organisms that bioturbate the sediments. Warmer temperatures lower the frost line, which thickens the active layer in the tundra and promotes the weathering of clay minerals. Therefore, these processes provide a higher influx of sediment and the preservation of the clay mineral $I + IS$ in the lake sediments.

Cold (glacial) periods (intervals B and D) are marked by the preservation of laminated sediments, lower sedimentation rates, a reduction in relative grain-size, and an increase in the percentage of chlorite clay mineral. Diminished mixing of the water column promotes anoxia at the sediment-water interface; preserving laminated sediments due to lack of bioturbating organisms. Persistent lake-ice and the thin active layer in the tundra limit the amount, size and character of sediments that enter the lake. In this environment, grain-size distribution is skewed to the finer GSD3 mode of sedimentation. Reduced weathering of clay minerals in the thin active layer results in the preservation of chlorite.

These records imply circumarctic teleconnections that are physically linked through atmospheric circulation (Brigham-Grette et al. 2007). To further validate these connections additional modeling of the geochronology on sedimentation rates must be completed, especially in marine isotopes stage 3.

References

Andersen DW, Wharton RA Jr, Squyres SW (1993) Terrigenous clastic sedimentation in Antarctic Dry Valley Lakes. Antarct Res Ser 59:71–81

Anderson PM, Lozhkin AV (eds) (2002) Late Quaternary vegetation and climate of Siberia and the Russian far east: a palynological and radiocarbon database. NOAA Paleoclimatology and North East Science Center, Magadan, pp 369

Anderson PM, Lozhkin AV, Brubaker LB (2002) Implications of a 24,000-yr palynological record for a Younger Dryas cooling and for boreal forest development in northeastern Siberia. Quaternary Res 57:325–333

Anderson PM, Edwards ME, Brubaker LB (2004) Results and paleoclimate implications of 35 years of paleoecological research in Alaska. Development in Quaternary Science: the quaternary period in the United States, vol I. pp 427–440

Al-Borno A, Tomson MB (1994) The temperature dependence of the solubility product constant of vivianite. Geochim Cosmochim Ac 58:5373–5378

Ariztegui D, Chondrogianni C, Lami A, Guilizzoni P, Lafargue EJ (2001) Lacustrine organic matter and the Holocene paleoenvironmental record of Lake Albano (central Italy). J Paleolimnol 26:283–292

Behl RJ (1995) Sedimentary facies and sedimentology of the Late Quaternary Santa Barbara Basin (ODP Site 893) Proc. O.D.P., Sci. Res., 146: part II, College Station, TX (Ocean Drilling Program), pp 295–308

Behl RJ, Kennett JP (1996) Brief interstadial events in the Santa Barbara Basin, NE Pacific, during the past 60 kyr. Nature 379:243–246

Belyi VF (1982) The El'gygytgyn lake basin—meteoritic crater or geological structure of the newest stage of the evolution of the Central Chukotka? [in Russian] Pacific Geology 5:85–91

Belyi VF, Chereshnev IA (eds) (1993) The nature of the El'gygytgyn Lake Hollow. [in Russian] Magadan FEB Russ Ac Sci, p 250

Belyi VF, Belya BV, Raikevich MI, (1994) Pliocene deposits of upstream of the Enmyvaam River and the age of impactogenesis in the El'gygytgyn Lake Hollow. [in Russian]. Magadan, NESRI FEB Russ Ac Sci, p 24

Berner RA (1971) Principles of chemical sedimentation. McGraw-Hill, New York, pp 270

Biscaye PE (1964) Distinction between kaolinite and chlorite in recent sediments by X-ray diffraction. Am Mineral 49:1281–1289

Blaise B (1989) Clay-mineral assemblages from late Quaternary deposits on Vancouver Island, southwester British Columbia, Canada. Quaternary Res 31:41–56

Brigham-Grette J, Melles M, Minuk PS (2007) Overview and significance of a 250 ka Paleoclimate Record from El'gygytgyn Crater Lake, NE Russia. J Paleolimnol DOI 10.1007/s10933-006-9017-6 (this issue)

Brigham-Grette J, Lozhkin AV, Anderson PM, Glushkova OY (2004) Paleoenvironmental conditions in Western Beringia before and during the Last Glacial Maximum. In: Madsen DB (ed) Northeast Asia and Beringia before the last glacial maximum. Univ. of Utah Press, Entering America, pp. 29–61

Chamley H (1989) Clay sedimentology. Springer-Verlag Berlin Heidelberg, Germany, 623 pp

Forman SL, Pierson J, Gómez J (2007) Luminescence geochronology for sediments from Lake El'gygytgyn, northeast Siberia, Russia: constraining the timing of paleoenvironmental events for the past 200 ka. J Paleolimnol DOI 10.1007/s10933-006-9024-7 (this issue)

Francus P (2001) Quantification of bioturbation in hemipelagic sediments via thin-sections image analysis. J Sediment Res 71:501–507

Francus P, Asikainen CA (2001) Sub-sampling unconsolidated sediments: a solution for the preparation of undisturbed thin-sections from clay-rich sediments. J Paleolimnol 26:323–326

Gale SJ, Hoare PG (1991) Quaternary sediments: petrographic methods for the study of unlithifed rocks. Belhaven Press, NY, 323 pp

Glushkova OYu (1993) In: Bely VF, Chereshnev IA (eds) The nature of the El'gygytgyn Lake Hollow. Russ Ac Sci, 26–48

Glushkova OYu, Smirnov VN (2007) Pliocene to Holocene geomorphic evolution and paleogeography of the El'gygytgyn Lake region, NE Russia. J Paleolimnol DOI 10.1007/s10933-006-9021-x (this issue)

Grootes PM, Stuiver M, White JWC, Johnsen SJ, Jouzel J (1993) Comparison of oxygen isotope records from the GISP2 and GRIP Greenland ice cores. Nature 366:552–554

Hu SF and Shemesh A (2003) A biogenic-silica δO^{18} record of climatic change during the last glacial-interglacial transition in southwestern Alaska. Quaternary Res 59:379–385

Imbrie J, Berger A, Boyle EA, Clemens SC, Duffy A, Howard WR, Kukla G, Kutzbach LC, Martinson J, McIntyre DG, Mix A, Molfino AC, Morley B, Peterson JJ, Pisias NG, Prell WL, Raymo ME, Shackleton NJ, Toggweiler JR (1993) On the structure and origin of major glaciation cycles, 2, The 100,000-year cycle. Paleoceanography 8:699–735

Last WM (2001) Textural analysis of lake sediments. In: Last WM, Smol JP (eds) Tracking environmental change using lake sediments: physical and chemical techniques. Kluwer Academic Publishers, Dordrecht, The Netherlands, pp 41–81

Layer PW (2000) Argon-40/argon-39 age of the El'gygytgyn impact event, Chichotka, Russia. Meteorit Planet Sci 581–599

Lozhkin AV, Anderson PM (1996) A late Quaternary pollen record from Elikchan 4 Lake, northeast Siberia. Geol Pac Ocean 12:609–616

Lozhkin AV, Anderson PM, Matrosova1 TV, Minyuk PS (2007) Vegetation and climate histories of Elgygytgyn Lake, Northeast Siberia. J Paleolimnol DOI 10.1007/s10933-006-9018-5 (this issue)

Malo BA (1997) Partial extraction of metals from aquatic sediments. Environ Sci Technol 277–282

Mackay AW, Battarbee RW, Flower RJ, Jewson D, Lees JA, Ryves DB, Sturm M (2000) The deposition and accumulation of endemic planktonic diatoms in the sediments of Lake Baikal and an evaluation of their potential role in climate reconstruction during the Holocene. Terra Nostra 9:34–48

Melles M, Brigham-Grette J, Glushodova OYu, Minyuk PS, Nowaczyk N, Hubberten HW (2007) Sedimentary geochemistry of a pilot core from Lake El'gygytgyn—a sensitive record of climate variability in the East Siberian Arctic during the past three climate cycles. J Paleolimnol DOI 10.1007/s10933-006-9025-6 (this issue)

Minyuk PS, Brigham-Grette J, Melles M, Borkhodoev VYa, Glushkova OYu (2007) Inorganic geochemistry of El'gygytgyn Lake sediments, northeastern Russia, as

an indicator of paleoclimatic change for the last 250 kyr. J Paleolimnol DOI 10.1007/s10933-006-9027-4 (this issue)

Moore DM, Reynolds RC Jr (1989) X-Ray Diffraction and the identification and analysis of clay Minerals. Oxford University Press, 332 pp

Mothersill JS (1996) The formation of vivianite-rich nodules in Lake Victoria. In: Johnson TC, Odada EO (eds) The Limnology, climatology and Paleoclimatology of the East African Lakes. Gordon and Breach Publ, Amsterdam, pp 53–548

Müller J (2000) Late Pliocene environmental history of SE Siberia as inferred from Lake Baikal sediments. Dissertation des Alfred-Wegener-Institus, Potsdam, Germany

Nealson KH (1997) Sediment bacteria: Who's there, what are they doing, and what's new? Annu Rev Earth Planet Sci 25:403–434

Niessen F, Gebhardt AC, Kopsc C, Wagner B (2007) Seismic investigation of the El'gygytgyn impact crater lake: preliminary results. J Paleolimnol DOI 10.1007/s10933-006-9022-9 (this issue)

Nolan M, Brigham-Grette J (2007) Basic hydrology, limnology, and meteorology of modern Lake El'gygytgyn, Siberia. J Paleolimnol DOI 10.1007/s10933-006-9020-y (this issue)

Nowaczyk NR, Minyuk PS, Melles M, Brigham-Grette J, Glushkova OYu, Nolan M, Lozhkin AV, Stetsenko TV, Andersen P, Forman SL (2002) Magnetostratigraphic results from impact crater Lake El'gygytgyn, North-eastern Siberia: a 300 kyr long high-resolution terrestrial paleoclimate record from the Arctic. Geophyss J Int 150:109–126

Nowaczyk NR, Melles M, Minyuk PS (2007) A revised age model for core PG1351 from Lake El'gygytgyn, Chukotka, based on magnetic susceptibility variations tuned to northern hemisphere insolation variations. J Paleolimnol DOI 10.1007/s10933-006-9023-8 (this issue)

Nriagu JO, Dell CI (1974) Diagenetic formation of iron phosphates in recent lake sediments. Am Mineral 59:943–946

Overpeck J, Hughen K Hardy D, Bradley R, Case R, Douglas M, Finney B, Gajewski K, Jacoby G, Jennings A, Lamoureux SK, Lasca A, MacDonald G, Moore J, Retelle M, Smith S, Wolfe A, Zienlinski G (1997) Artic environmental change of the last four centuries. Science 278:1251–1256

Peck JA, King JW, Colman SM, Kravchinsky VA (1994) A rock-magnetic record from Lake Baikal, Siberia: evidence for Late Quaternary climate change. Earth Planet Sci Lett 221–238

Perren B, Bradley RS, Francus P (2003) Rapid lacustrine response to recent High Arctic warming: a diatom record from Sawtooth Lake, Ellesmere Island, Nunavut. Arct Antarct Alp Res 35:271–278

Petschick R, Kuhn G, Gingele F (1996) Clay mineral distribution in surface sediments of the South Atlantic: sources, transport, and relation to oceanography. Mar Geol 130:203–229

Priscu JP, Fritsen CH, Adams EE, Giovannoni SJ, Pearl HW, McKay CP, Doran PT, Gordon DA, Lanoil BD, Pinckney JL (1998) Perennial Antarctic lake ice: an oasis for life in a polar desert. Science 280:2095–2098

Sutinen R, Haavikko P, Hanninen P (1993) Consistency of Particle size analysis of Geological Earth materials and the effect of sample preparation procedures on reproducibility. Geol Surv Finland Spec Pap 18:63–72

Velde B (1995) Composition and mineralogy of clay minerals. In: Velde B (eds) Origin and mineralogy of clays: clays and the environment. Springer-Verlag, New York, pp 8–42

Vigliotti L, Capotondi L, Torii M (1999) Magnetic properties of sediments deposited in suboxic-anoxic environments: relationships with biological and geochemical proxies. In: Tarling DH, Turner, P (eds) Paleomagnetism and Diagenesis in Sediments. Geol Soc London Spec Pub 151:71–83

Vologina EG, Granin NG, Lomonosova TK, Vorobyeva SS, Kulikova NA, Kalashnikova IA, Granina LZ (2003) Input of silt-sand material to the central part of southern lake Baikal by ice transportation. BAIK-SED-2, Gent University, Belgium, pp 17–18

Vologina E, Granin N, Vorobyeva S, Francus P, Lomonosova T, Kalashnikova I, Granina L (2005) Ice transportation of sand-silt material in southern lake Baikal. Geol Geofiz 46(4):186–192

Wetzel RG (1983) Limnology, 2nd edn. Saunders College Publishing, Philadelphia, 767 pp

Yuretich R, Melles M, Sarta B, Grobe H (1999) Clay minerals in the sediments of Lake Baikal; a useful climate proxy. J Sediment Res 69:588–596